

## Anisotropy of light extraction from two-dimensional photonic crystal light-emitting diodes

Chun-Feng Lai, H. C. Kuo, C. H. Chao, H. T. Hsueh, J.-F. T. Wang, W. Y. Yeh, and J. Y. Chi

Citation: [Applied Physics Letters](#) **91**, 123117 (2007); doi: 10.1063/1.2789399

View online: <http://dx.doi.org/10.1063/1.2789399>

View Table of Contents: <http://scitation.aip.org/content/aip/journal/apl/91/12?ver=pdfcov>

Published by the [AIP Publishing](#)

---

### Articles you may be interested in

[Light extraction from GaN-based light emitting diode structures with a noninvasive two-dimensional photonic crystal](#)

Appl. Phys. Lett. **94**, 023101 (2009); 10.1063/1.3067837

[Enhanced light extraction from GaN-based green light-emitting diode with photonic crystal](#)

Appl. Phys. Lett. **91**, 181109 (2007); 10.1063/1.2804005

[Fabrication of two-dimensional photonic crystal patterns on GaN-based light-emitting diodes using thermally curable monomer-based nanoimprint lithography](#)

Appl. Phys. Lett. **91**, 091106 (2007); 10.1063/1.2776980

[Enhanced light extraction from GaN-based light-emitting diodes with holographically generated two-dimensional photonic crystal patterns](#)

Appl. Phys. Lett. **87**, 203508 (2005); 10.1063/1.2132073

[Efficiency enhancement in a light-emitting diode with a two-dimensional surface grating photonic crystal](#)

Appl. Phys. Lett. **84**, 457 (2004); 10.1063/1.1644033

---

The advertisement features a dark blue background with white and orange text. At the top left, it reads 'NEW! Asylum Research MFP-3D Infinity™ AFM' in large white letters, followed by 'Unmatched Performance, Versatility and Support' in orange. On the right, the Oxford Instruments logo is shown with the tagline 'The Business of Science®'. Below the text are four images: a textured surface, a circular pattern, a grid of small squares, and the MFP-3D Infinity AFM instrument itself. Text descriptions are placed around these images: 'Stunning high performance' next to the textured surface, 'Simpler than ever to GetStarted™' next to the circular pattern, 'Comprehensive tools for nanomechanics' next to the grid, and 'Widest range of accessories for materials science and bioscience' next to the AFM instrument.

## Anisotropy of light extraction from two-dimensional photonic crystal light-emitting diodes

Chun-Feng Lai and H. C. Kuo<sup>a)</sup>

*Department of Photonics and Institute of Electro-Optical Engineering, National Chiao-Tung University, Hsinchu, 300 Taiwan, Republic of China*

C. H. Chao, H. T. Hsueh, J.-F. T. Wang, W. Y. Yeh, and J. Y. Chi

*Electronics and Opto-Electronics Research Laboratories, Industrial Technology Research Institute, Hsinchu, 310 Taiwan, Republic of China*

(Received 8 August 2007; accepted 4 September 2007; published online 20 September 2007)

Anisotropic light extraction of photonic crystal (PhC) light-emitting diodes in the azimuthal direction has been investigated with an annular structure of triangular PhC lattice. The optical images of the photoluminescence light extraction are obtained with laser excitation. For increasing lattice constant, sixfold symmetric patterns with varying numbers of petals in multiples of six are observed and analyzed. A map of the anisotropy for various lattice constants and numerical apertures is constructed. Several features of light propagations associated with the PhC are observed including the focusing and collimating behaviors. © 2007 American Institute of Physics.

[DOI: 10.1063/1.2789399]

Recently, photonic crystal (PhC) has attracted a great deal of attention for the possibility to improve the extraction efficiency of light-emitting diodes (LEDs).<sup>1-6</sup> To optimize the device performance for a specific system, detailed knowledge of the light extraction, especially the angular distribution, is required. Angular variations of light extraction in the zenith (vertical) direction have been investigated.<sup>7</sup> However, the angular distribution in the azimuthal (in-plane) direction has not been examined in detail.

In this paper, we present the direct imaging of the in-plane angular distribution of the extracted light using a specially designed structure. A map of the anisotropy for various lattice constants and numerical apertures is constructed. Several features particular to the PhC properties have also been directly observed. These results can be used for the device optimization to take full advantage of the PhC.

The GaN epitaxial structure used for the present study was grown by metal-organic chemical vapor deposition, consisting of a 1- $\mu\text{m}$ -thick GaN buffer on a *c*-sapphire substrate, a 2  $\mu\text{m}$  bottom *n*-GaN layer, a 100 nm InGaN/GaN multiple quantum well (MQW) region, and a 130-nm-thick top *p*-GaN current spreading layer, as shown in Fig. 1(a). The annular region of triangular PhC with an inner/outer diameter of 100/200  $\mu\text{m}$  was patterned by electron-beam lithography. Holes were then etched into the top *p*-GaN layer using inductively coupled plasma dry etching to a depth  $t = 120$  nm. The orientation of the triangular PhC is fixed in space and the ratio of hole diameter  $d$  to lattice constant  $a$  is also fixed to 0.6 to provide the consistent band structure.

After fabrication, the wafer is examined with a micro-photoluminescence ( $\mu$ -PL) system. A 325 nm He-Cd laser beam normally incidents into the central area of the ring and excites the wavelength  $\lambda = 470$  nm PL light in the MQW active region. The laser power used is about 3.2 mW and focused to a spot of about 5  $\mu\text{m}$ . A 15 $\times$  objective with numerical aperture (NA) of 0.32 is used to collect the on-axis emission signal from the sample and formed a high-

resolution image with a digital charge-coupled device (CCD) camera after filtering out the laser light.

Figure 2 shows the CCD images for samples with lattice constants  $a$  of 300, 450, 600, and 750 nm corresponding to  $a/\lambda$  of 0.63, 0.96, 1.33, and 1.59, respectively. The bright region that appeared in the center of all images is due to the unguided PL light. The petals in the PhC regions are due to the guided light that travel to the surrounding PhC region and get extracted. It can be seen that the angular distribution of the extracted light is strongly anisotropic. As  $a/\lambda$  increases, the increasing number of petals in multiples of six appears in a sixfold rotational symmetric pattern, indicating for certain directions, that stronger extraction with a focusing behavior is observed.

The observed anisotropy in Fig. 2 may be caused by either the coupling into the PhC region, which has been reported before,<sup>8</sup> or by the diffraction of the light after coupling into the PhC. According to our finite-difference time domain (FDTD) simulation, a coupling anisotropy of only  $<5\%$  are expected from the present shallow etch structure and high  $a/\lambda > 0.6$ . Therefore, the observed anisotropy is primarily due to the diffraction of the guided PL light of the PhC lattice into air and picked up by the microscope objective.

The anisotropy due to diffraction can be explained by considering the Ewald construction in the reciprocal lattice. For simplicity, PhC is treated as a two-dimensional in an overall three-dimensional structure as is commonly done.<sup>7</sup> Figure 3 shows the projection of the Ewald sphere on the waveguiding plane. The three circles in the figure correspond to the waveguide mode circle (blue dash line) with radius  $k = 2n\pi/\lambda$ , where  $n$  is the effective refractive index of the guided wave, the air disk (red solid line), with radius  $k_0 = 2\pi/\lambda$ , and the inner circle (green solid line) corresponds to  $\text{NA} = \sin \theta$ , where  $\theta$  is the acceptance angle for the optics used for the observation. The in-plane component of the resultant wavevector can couple to the reciprocal lattice vectors. If the resultant vector falls inside the air circle, the diffracted light can escape into air. However, to be picked up

<sup>a)</sup>Electronic mail: hckuo@faculty.nctu.edu.tw

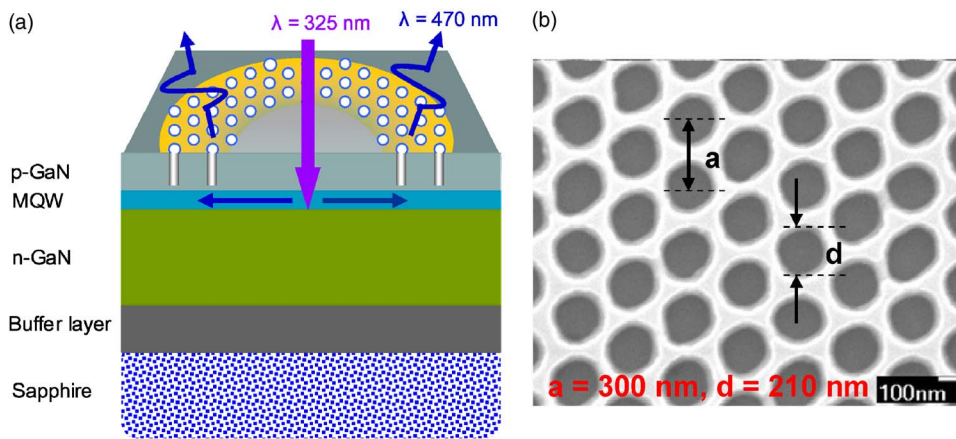


FIG. 1. (Color online) (a) Annual structure and the light generation, waveguiding, and extraction in the present structure, (b) Scanning electron microscope micrograph of the PhC region.

with the objective lens, the diffracted light must fall within the NA circle. Using Ewald construction, this rule becomes simply to determine whether a reciprocal lattice point appears inside the particular circles. This simple rule provides an explanation of the observed pattern of light extraction. It can also be used to define the conditions for observing of varying numbers of petals as a function of NA.

Figure 4 shows the boundary separating the regions with different numbers of petals along with our observations with  $NA=0.32$  and  $a/\lambda=0.63$ . As lattice constant increases above cutoff (line  $G_{\Gamma-M}^+$  in Fig. 4), light propagation in the  $\Gamma$ - $M$  direction will start to be extracted [Fig. 3(a)]. As  $a/\lambda$  increases, the resultant wavevector after coupling to  $G_{\Gamma-M}$  falls inside the NA circle [Fig. 3(b)]. However, the opposite is true in the  $\Gamma$ - $K$  direction [Fig. 3(c)]. Therefore, a pattern with six petals pointing to the  $\Gamma$ - $M$  direction is observed. As  $a/\lambda$  increases further, the resultant wavevector after coupling to  $G_{\Gamma-M}$  may fall short of the NA circle and will not be observed. Figure 3(a) [Fig. 3(b)] illustrates the situation when

the reciprocal points almost start to appear (disappear) inside the NA circle. Thus there is a range of  $a/\lambda$  that the resultant wavevector can fall into the NA circle in a particular direction. This is represented as solid and dashed lines marked as  $G_{\Gamma-M}^+$  and  $G_{\Gamma-M}^-$  in Fig. 4.

Since the present thick epitaxial layer of  $3.3 \mu\text{m}$ , the waveguiding is multimode. Every waveguiding mode can couple with the reciprocal vectors to form two lines in the same fashion described above. When plotted on the map, these multimodes will appear as a band of lines. For clarity, only the first and the last modes with mode number  $m$  are shown in Fig. 4. The two outmost lines,  $G_{\Gamma-M}^+$  and  $G_{\Gamma-M}^-$ , define the boundary of the possible  $a/\lambda$ 's for all the modes that can fall into NA circle after coupling to  $G_{\Gamma-M}$ .

For still larger lattice constant of  $a/\lambda > 2/n$ , coupling to the second nearest vector  $G_{\Gamma-K}$  becomes possible and six more petals appear representing six equivalent  $\Gamma$ - $K$  directions. The boundary for all the coupling to  $G_{\Gamma-K}$  can be drawn in the same way as above and is indicated by  $G_{\Gamma-K}^+$  and  $G_{\Gamma-K}^-$  (fall outside Fig. 4, not shown). In the overlap of the two regions, 12 petals will be obtained, pointing alternately to the  $\Gamma$ - $M$  and  $\Gamma$ - $K$  directions. For even larger lattice constants, coupling to the third and fourth nearest lattice points, with the vector length two times the  $G_{\Gamma-M}$  (line  $2G_{\Gamma-M}^+$ ) and  $G_{\Gamma-M}^- + G_{\Gamma-K}$  (line  $G_{\Gamma-M}^+ + G_{\Gamma-K}^+$ ) is possible and the number of petals increases to 24. Also there are regions where no dif-

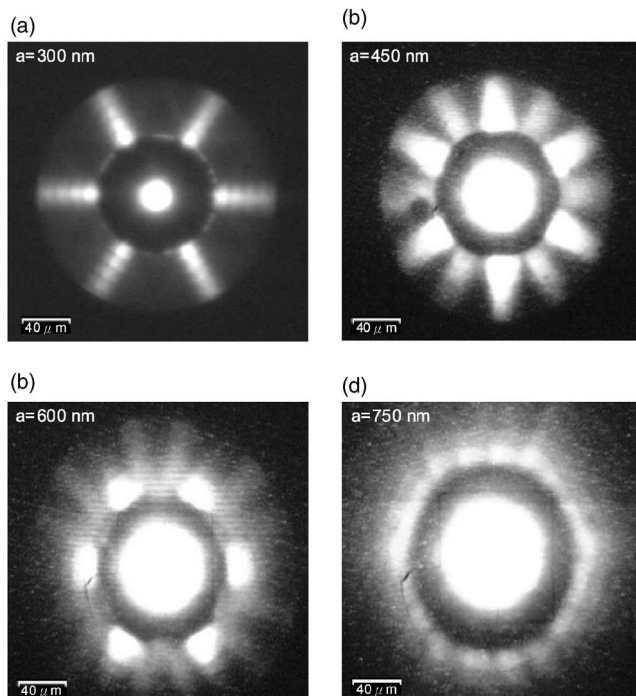


FIG. 2. CCD images for various lattice constants of (a) 300, (b) 450, (c) 600, and (d) 750 nm. The central bright region in all the photos is due to the unguided PL light excited by the focused laser beam impinging normally in the center.

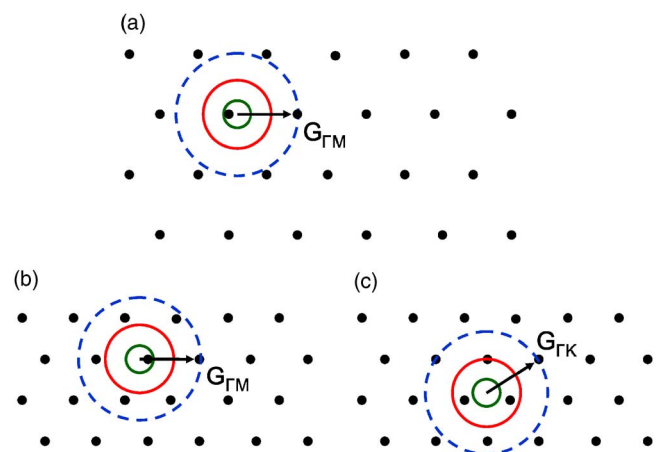


FIG. 3. (Color online) Ewald construction for (a) the resultant wavevector just entering the NA circle, (b) coupling in the  $G_{\Gamma-M}$  direction for  $a = 300 \text{ nm}$  showing the resultant wavevector almost leaving the NA circle, and (c) coupling in the  $G_{\Gamma-K}$  direction for  $a=300 \text{ nm}$  showing no light can escape into the NA.



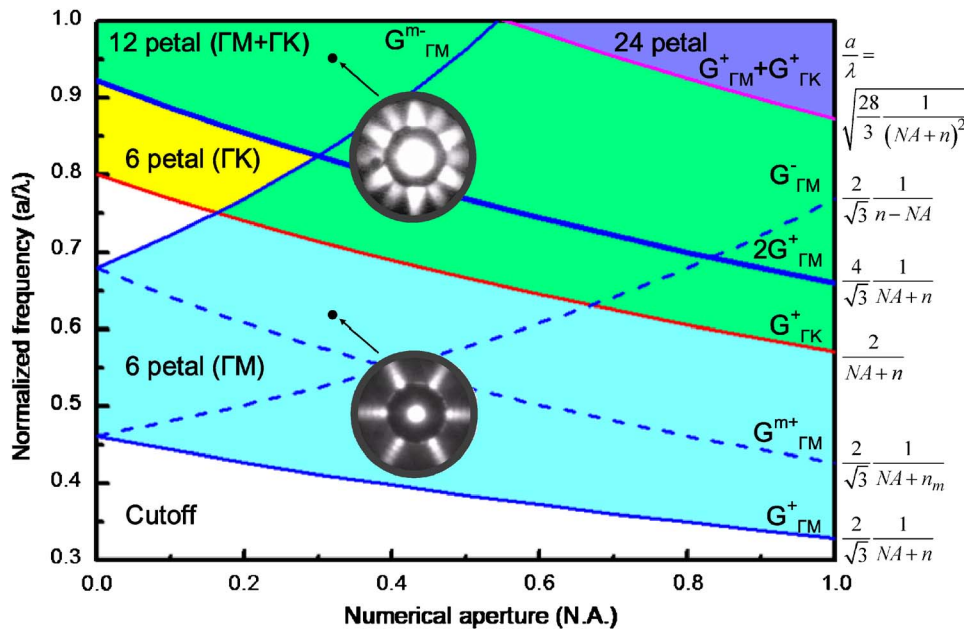


FIG. 4. (Color online) Map for the azimuthal anisotropy of the triangular lattice as a function of NA. The regions of various petals are shown with different colors. The directions of the petals are shown in parentheses. The “+” and “-” signs indicate the lower and upper boundaries for the regions.

fraction appears, corresponding to the light escaping the surface with angles larger than NA. The formulas for the boundary between regions with different numbers of petals can be readily derived and are shown in Fig. 4.

It is also observed that the interference fringes are superimposed on the patterns, as shown in Fig. 2(a). The spacing of the fringes stays the same for all propagation directions and lattice constants. The origin of the fringes is most likely due to the multimode interferences (MMIs) of the modes traveling in the waveguide formed by the epitaxial film on top of the sapphire. For a quantitative comparison, the spacing due to MMI are calculated with the formula  $s = 4n_e W^2 / (N\lambda_0)$ .<sup>9</sup> Using an epitaxial thickness  $W$  of  $3.23 \mu\text{m}$ , a total mode number  $N$  of 25 modes supported by the waveguide before the leakage into the sapphire substrate, and the effective index  $n_e$  of 2.5, the spacing is determined to be about  $9 \mu\text{m}$ , or  $9.8 \mu\text{m}$  with the Goose-Hahnchen correction. This value is reasonably close to the measured fringe spacing of  $10.4 \mu\text{m}$ , considering the inaccuracy of the parameters in the formula.

In addition to the observed number of petals, the shape of the individual petals is worth commenting on: The petals inside the annular regions are convergent in shape, instead of the expected divergent shape. Such a shape may be due to the dispersion of the band structure. For the 12-petals pattern shown in Fig. 2(b), it is seen that the focusing is stronger in the  $\Gamma$ - $M$  directions than the  $\Gamma$ - $K$  directions which may reflect the different dispersion properties of the two directions. In addition to the anisotropy, the emitted light are polarized with a TE/TM ratio larger than 10. The intensity of the extracted light decreases with a decay length of  $70$ – $90 \mu\text{m}$ , depending on the orientation and the holes size; this value is

in the same range of that reported in Ref. 7. The discussion of these details will be reported elsewhere.

In conclusion, optical images of the anisotropy in the azimuthal direction of GaN PhC LEDs are obtained using annular structure with triangular lattice. The presented imaging approach can be used to study the propagation of light in the PhC slabs and provides information important for designing LED and other photonic devices.

The authors gratefully acknowledge Dr. S. C. Wang at National Chiao-Tung University (NCTU) and Y. S. Liu at National Tsing-Hua University (NTHU) in Taiwan for their technical support. This work is supported by the National Nanotechnology Program of Taiwan, R.O.C., and the MOE ATU program and, in part, by the National Science Council of the Republic of China under Contract Nos. NSC 95-2120-M-009-008, NSC 95-2752-E-009-007-PAE, and NSC 95-2221-E-009-282.

<sup>1</sup>E. F. Schubert, *Light-Emitting Diodes* (Cambridge University Press, Cambridge, 2003).

<sup>2</sup>H. Ichikawa and T. Baba, *Appl. Phys. Lett.* **84**, 457 (2004).

<sup>3</sup>T. N. Oder, K. H. Kim, J. Y. Lin, and H. X. Jiang, *Appl. Phys. Lett.* **84**, 466 (2004).

<sup>4</sup>J. J. Wierer, M. R. Krames, J. E. Epler, N. F. Gardner, and M. G. Craford, *Appl. Phys. Lett.* **84**, 3885 (2004).

<sup>5</sup>J. Shakyia, K. H. Kim, J. Y. Lin, and H. X. Jiang, *Appl. Phys. Lett.* **85**, 142 (2004).

<sup>6</sup>C. H. Chao, S. L. Chuang, and T. L. Wu, *Appl. Phys. Lett.* **89**, 091116 (2006).

<sup>7</sup>A. David, C. Meier, R. Sharma, F. S. Diana, S. P. DenBaars, E. Hu, S. Nakamura, and C. Weisbuch, *Appl. Phys. Lett.* **87**, 101107 (2005).

<sup>8</sup>A. Martinez and J. Marti, *Phys. Rev. B* **71**, 235115 (2005).

<sup>9</sup>R. Ulrich and G. Ankele, *Appl. Phys. Lett.* **27**, 337 (1975).